Water Science and Engineering, 2014, 7(3): 250-266
doi:10.3882/j.issn.1674-2370.2014.03.002
http://www.waterjournal.cn
e-mail: wse2008@vip.163.com

Climate change trend and its effects on reference evapotranspiration at Linhe Station, Hetao Irrigation District

Xu-ming WANG, Hai-jun LIU*, Li-wei ZHANG, Rui-hao ZHANG

College of Water Sciences, Beijing Normal University, Beijing 100875, P. R. China

Abstract: Linhe National Meteorological Station, a representative weather station in the Hetao Irrigation District of China, was selected as the research site for the present study. Changes in climatic variables and reference evapotranspiration (ET_0) (estimated by the Penman-Monteith method) were detected using Mann-Kendall tests and Sen's slope estimator, respectively. The authors analyzed the relationship between the ET_0 change and each climatic variable's change. From 1954 to 2012, the air temperature showed a significant increasing trend, whereas relative humidity and wind speed decreased dramatically. These changes resulted in a slight increase in ET_0. The radiative component of total ET_0 increased from 50% to 57%, indicating that this component made a greater contribution to the increase in total ET_0 than the aerodynamic component, especially during the crop growing season (from April to October). The sensitivity analysis showed that ET_0 in Hetao is most sensitive to mean daily air temperature (11.8%), followed by wind speed (−7.3%) and relative humidity (4.8%). Changes in sunshine duration had only a minor effect on ET_0 over the past 59 years.

Key words: *climatic variables; reference evapotranspiration; change trend; Mann-Kendall test; sensitivity analysis*

1 Introduction

Climate change is occurring worldwide (IPCC 2007) and may cause major changes in climatic variables such as precipitation, air temperature, relative humidity, and solar radiation (Haskett et al. 2000). It is expected to cause changes in the hydrological cycle by affecting precipitation and evaporation (Bates et al. 2008; Huntington 2006; Yu et al. 2013). These changes will also affect crop evapotranspiration and have major implications for irrigation management (Zhang et al. 2011b).

It has been confirmed that trends in climatic variables vary from place to place. In the French Mediterranean, Chaouche et al. (2010) reported increases in annual mean temperature and annual potential evapotranspiration, but no trend in annual precipitation. In southern Spain,

This work was supported by the National Natural Science Foundation of China (Grant No. 51179005) and the Special Fund for Public Welfare Industry of the Ministry of Water Resources of China (Grant No. 201401036).
*Corresponding author (e-mail: *shanxilhj@bnu.edu.cn*)
Received Mar. 18, 2014; accepted May 2, 2014

Espadafor et al. (2011) detected increasing trends in air temperature and solar radiation and a decreasing trend in relative humidity.

In recent years, numerous studies have been conducted to examine the potential impact of climate change on reference evapotranspiration (ET_0). These studies show that trends in ET_0 vary with climatic conditions and regions (Rim 2009). Darshana and Pandey (2013) reported significant annual, seasonal, and monthly (for almost all months) decreasing trends in ET_0 in the Tons River Basin in Central India, and the magnitude of decrease of annual ET_0 varied from –1.75 to –8.98 mm/year. Similarly, a significant decline in ET_0 (–0.36 mm/year) was observed on the Platte River Basin in central Nebraska, USA (Irmak et al. 2012). These authors attributed the decline in ET_0 to significant ($P \leq 0.05$) increases in precipitation (0.87 mm/year) that resulted in significant reductions in net radiation (–0.0032 MJ/(m·year)) (Irmak et al. 2012). In Iran, significant decreasing trends in ET_0 have been recorded in most regions, but increasing trends have also been found in some areas, especially in recent years (Kousari et al. 2013; Tabari et al. 2011; Talaee et al. 2014). Tabari et al. (2012) showed that in the west and southwest of Iran, wind speed was the dominant factor affecting ET_0. Statistically significant increases in ET_0 (up to 3.5 mm/year) were detected in southern Spain by Espadafor et al. (2011) and were attributed to increases in air temperature and solar radiation and decreases in relative humidity.

In China, climatic variation and its effects on ET_0 have been studied at the national and regional scales. At the national scale, mean annual ET_0 decreased significantly by –14.35 mm per decade from 1960 to 1992 and increased by 22.40 mm per decade from 1993 to 2011 (Zhang et al. 2013). In contrast, at the regional scale, trends in ET_0 varied with location. Decreasing trends in ET_0 were detected across the entire Yangtze River Basin in central China (Xu et al. 2006), on the Tibetan Plateau of Northwest China (Yang et al. 2009), in the Pearl River Basin of southeastern China (Zhang et al. 2011a), in the Haihe River Basin of northern China (Tang et al. 2011), in Yunnan Province in southwestern China (Fan and Thomas 2013), and in the arid regions of northwestern China (Huo et al. 2013). Increasing trends in ET_0 were found in the middle and upper Yellow River Basin (Zhang et al. 2011a). Additionally, Liang et al. (2006) reported that ET_0 showed an increasing tendency from 1951 to 2000 on the western Songnen Plain in northern China.

Studies have indicated that climatic variables that strongly influence ET_0 also vary from one region to another. In the Haihe River Basin of northern China, Tang et al. (2011) attributed a decrease in ET_0 at a rate of –1.0 mm/year to decreases in net radiation (–0.9 mm/year), vapor pressure deficit (–0.5 mm/year), wind speed (–1.3 mm/year), and air temperature (–1.7 mm/year). In the Yangtze River Basin, reductions in ET_0 and pan evaporation were mainly caused by significant decreases in net total radiation and wind speed (Gong et al. 2006). In northwestern China, Huo et al. (2013) found that ET_0 was most sensitive to wind speed, followed by relative humidity, temperature, and radiation. In contrast, in the western Songnen Plain in northern China, increasing trends in ET_0 were mainly attributed to decreasing humidity and increasing air temperature (Liang et al. 2006, 2008). Similarly, Ren et al. (2012) found that the air temperature and relative humidity are the key factors that affect potential evaporation at different time scales in the Hailar region in Northeast China. At the national scale, decreasing trends in ET_0 in most regions of China are driven by changes in vapor pressure deficit, maximum daily temperature, radiation, and wind speed (Liu et al. 2012).

The Hetao Irrigation District is located in the arid region of northern China and is suffering a serious water shortage. Due to a lack of precipitation (precipitation of about 150 mm/year), crops are always irrigated with water from the Yellow River. With increasing demand for water caused by economic development and better quality of life, water allocation for irrigation in the Hetao Irrigation District will be reduced from 5.2 billion m^3/year to 4.0 billion m^3/year over the 2020s according to a plan created by the Yellow River Water Conservancy Commission (Xu et al. 2010) that includes the adoption of various water-saving technologies and optimal irrigation scheduling. Generally, irrigation scheduling depends on precipitation rates and crop water requirements. The latter is generally estimated using a crop coefficient and ET_0 (Allen et al. 1998). Therefore, understanding climate change trends and their effects on ET_0 is important for water resource management and sustainable agricultural development in Hetao. To our knowledge, there are few studies that comprehensively examine climatic variation and its effects on ET_0 in Hetao. The main contribution of this study is finding the climate and ET_0 changes in the Hetao region.

The objectives of this study were (1) to analyze changes in climatic variables and ET_0 from 1954 to 2012 in Hetao and (2) to identify the key factors that most strongly influence ET_0 using a sensitive analysis. Results from this study will provide important information for further studies on climatic change and irrigation scheduling in the Hetao Irrigation District.

2 Data and methods

2.1 Site and data

The study area is situated in the center of the Hetao Irrigation District in northern China. All meteorological data used in this study were obtained from the Linhe National Meteorological Station, located in the center of the Hetao Irrigation District (40°45′N, 107°25′E, and 1039.3 m above sea level). Considering the relatively flat field in the Hetao Irrigation District and the center position of this meteorological station, the Linhe Station was used as a representative station in this study. Meteorological data were obtained for the period from 1954 to 2012 for atmospheric pressure; daily precipitation; mean (T_{ave}), maximum (T_{max}), and minimum (T_{min}) temperatures; mean relative humidity; mean wind speed; and sunshine hours. A summary of climate conditions is listed in Table 1.

Table 1 Summary of climatic data from 1954 to 2012 at Linhe Station

Item	Mean daily value			Annual total value		
	Air temperature (℃)	Relative humidity (%)	Wind speed (m/s)	Sunshine hours (h/year)	Precipitation (mm/year)	ET_0 (mm/year)
Maximum	39.4	98.0	13.7	3 585	190	1 183
Minimum	–35.3	7.0	0.0	2 811	46	987
Average	7.8	48.9	2.3	3 156	105	1 095

2.2 Methods

2.2.1 Reference evapotranspiration

Reference evapotranspiration (ET_0) was calculated using the United Nations Food and Agriculture Organization (FAO) Penman-Monteith (hereafter denoted as PM) method. The formula for the PM method is as follows (Allen et al. 1998):

$$ET_0 = \frac{0.408\varDelta\left(R_{\mathrm{n}} - G\right) + \gamma \dfrac{900}{\left(T + 273\right)} U_2\left(e_{\mathrm{s}} - e_{\mathrm{a}}\right)}{\varDelta + \gamma\left(1 + 0.34U_2\right)} \tag{1}$$

where ET_0 is the reference evapotranspiration (mm/d); R_{n} is the net radiation (MJ/(m^2·d)); G is the soil heat flux (MJ/(m^2·d)), which can be neglected at daily intervals (Allen et al. 1998); γ is the psychrometric constant (kPa/℃); T is the average air temperature (K); U_2 is the wind speed measured at 2 m above the ground surface (m/s); $\varDelta$ is the slope of the saturation vapor pressure curve at a given air temperature (kPa/℃); and e_{s} and e_{a} are the saturation and actual vapor pressure, respectively (kPa). The value of $e_{\mathrm{s}} - e_{\mathrm{a}}$ is also called the vapor pressure deficit (VPD).

ET_0 has two components: the radiative component $ET_{0\mathrm{R}}$ and the aerodynamic component $ET_{0\mathrm{a}}$, expressed as the first and second parts, respectively, of the numerator on the right side of Eq. (1). Thus, Eq. (1) can be rewritten as

$$ET_0 = ET_{0\mathrm{R}} + ET_{0\mathrm{a}} \tag{2}$$

$$ET_{0\mathrm{R}} = \frac{0.408\varDelta\left(R_{\mathrm{n}} - G\right)}{\varDelta + \gamma\left(1 + 0.34U_2\right)} \tag{3}$$

$$ET_{0\mathrm{a}} = \frac{\gamma \dfrac{900}{\left(T + 273\right)} U_2\left(e_{\mathrm{s}} - e_{\mathrm{a}}\right)}{\varDelta + \gamma\left(1 + 0.34U_2\right)} \tag{4}$$

$ET_{0\mathrm{R}}$ represents the reference evapotranspiration that would be obtained if the heat budget of a surface were determined by radiation alone. This condition tends to be satisfied when short, well-watered reference vegetation is exposed to bright sunshine, humid air, and a light wind. $ET_{0\mathrm{a}}$ is the reference evapotranspiration imposed by the environment when the surface is fully coupled with the prevailing weather. This condition tends to be satisfied when short, well-watered reference vegetation is exposed to high wind speeds and a large VPD. Therefore, $ET_{0\mathrm{R}}$ and $ET_{0\mathrm{a}}$ were estimated separately in this study, and their individual contributions to ET_0 were calculated.

2.2.2 Sensitivity analysis

A sensitivity analysis was used to identify the climatic variables that most strongly influence ET_0 by following the method proposed by Möller et al. (2004). The process of the sensitivity analysis was as follows: (1) Mean values of air temperature, relative humidity, wind speed, and sunshine hours were calculated for each day of the year using climatic data from 1954 to 1960 (hereafter referred to as the 1950s, the first decade of the whole study period), and the corresponding daily ET_0 values were calculated using the mean daily values for the 1950s. The mean daily value for each climatic variable and daily ET_0 for the 1950s were set as the reference climatic variables and ET_0. The same method was used to calculate the mean values of each climatic variable for each day of the year using data from 2006 to 2012 (hereafter referred to as the 2000s), and the corresponding daily ET_0 was also estimated. (2) Sensitivity of ET_0 to changes in each climatic variable was analyzed by setting the climatic parameters of air temperature, relative humidity, wind speed, and sunshine hours (see Eqs. (1) through (4)) to their measured values from the 2000s and setting the other climatic parameters to their measured values from the 1950s. (3) A comparison of ET_0 values was performed by replacing the values of each variable from the 2000s (see Step 2) with the ET_0 values calculated from the 1950s data (see Step 1) to identify the variables with the strongest effect on ET_0.

2.2.3 Mann-Kendall test

The Mann-Kendall test is one of the most widely used non-parametric tests for detecting significant trends in climatic variables and ET_0 from time series data (Hamed 2008; Liang et al. 2010; Liu et al. 2014). Hence, in this study, the trends of climatic variables, ET_0, and irrigation water requirements were tested using the Mann-Kendall test. Detailed information related to the Mann-Kendall test can be found in studies published by Hamed (2008), Liang et al. (2010), and Liu et al. (2014).

2.2.4 Sen's slope estimator

If a data time series shows a linear trend, the true slope (change per unit of time) can be estimated using a simple nonparametric procedure given by Sen (1968). The Sen's slope estimator, *b*, is determined as follows:

$$b = \text{Median}\left(\frac{x_j - x_i}{j-1}\right) \qquad \forall i < j \tag{5}$$

where x_j and x_i are two generic sequential data values of a variable. For a time series of annual (crop growing seasonal or monthly) values, *b* represents the annual (crop growing seasonal or monthly) increment under the hypothesis of a linear trend. The *b* estimator approximates the true slope of the trend, which can slightly differ from the slope of the trend line obtained by linear regression.

Mann-Kendall tests and Sen's slope estimator calculations for monthly, seasonal, and annual mean data series for the meteorological variables and ET_0 values were performed using the EXCEL-based software MAKESENS 1.0 developed by Salmi et al. (2002).

3 Results and discussion

3.1 Trends in climatic variables and ET_0

Fig. 1 describes trends in T_{max}, T_{min}, T_{ave}, relative humidity, VPD, wind speed, annual total sunshine hours, and solar radiation at the Linhe Station from 1954 to 2012. For temperature, relative humidity, VPD, and wind speed, each point in the figure represents an annual mean value. For sunshine hours and solar radiation, each point represents the annual total value.

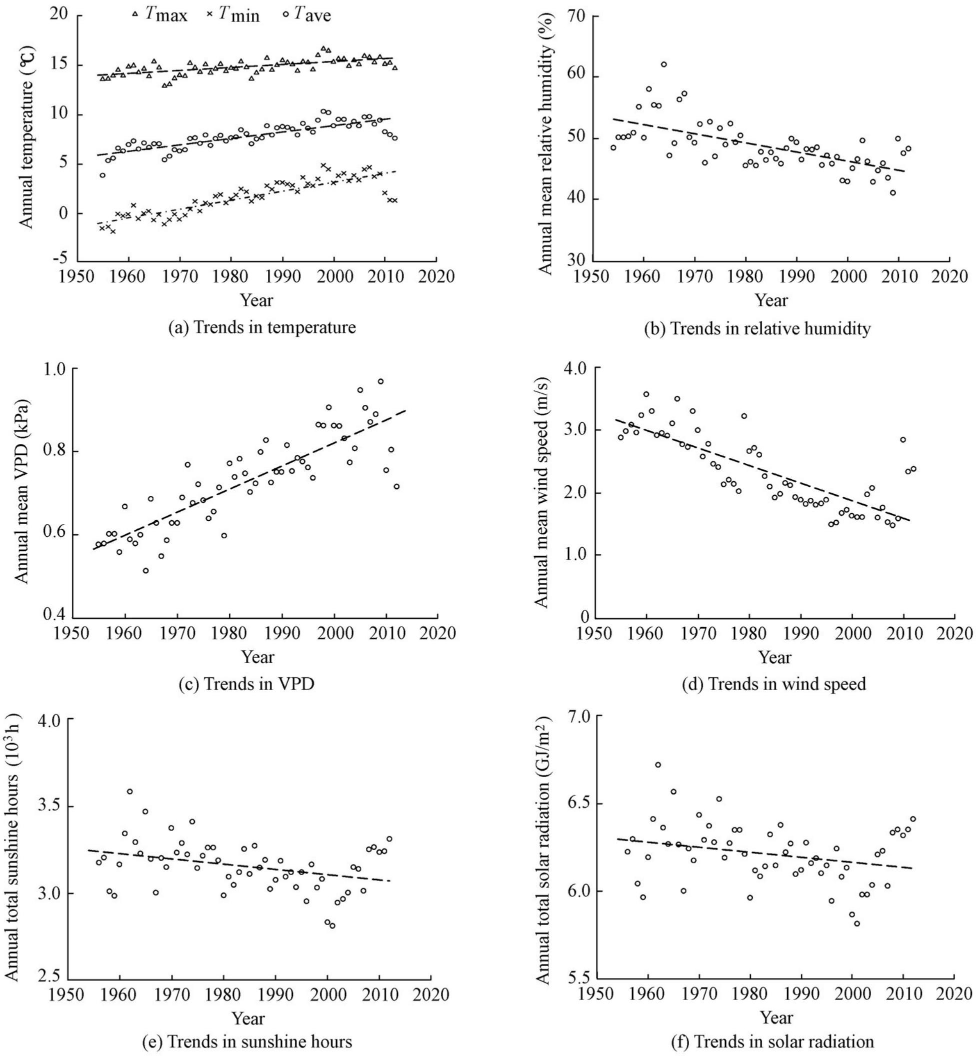

Fig. 1 Trends in climatic variables from 1954 to 2012

Sen's slope for each climatic variable and ET_0 and the corresponding statistical tests for linear rates of change (Mann-Kendall tests) are shown in Table 2.

Table 2 Sen's slope of linear trends in monthly, crop growing seasonal (April to October), and annual means for each climatic variable and ET_0 for 1954 to 2012

Time period	Change of Sen's slope for different variables per day								
	T_{max} (℃)	T_{min} (℃)	T_{ave} (℃)	Relative humidity (%)	VPD (kPa)	Wind speed (m/s)	Sunshine hours (h)	Solar radiation (MJ/m^2)	ET_0 (mm)
Jan.	0.011	0.099^{***}	0.068^{***}	0.055	0.001^{+}	-0.029^{***}	-0.014^{**}	-0.011^{**}	-0.003^{***}
Feb.	0.039^{+}	0.127^{***}	0.091^{***}	0.042	0.001^{**}	-0.035^{***}	-0.017^{**}	-0.017^{**}	0.000
Mar.	0.011	0.094^{***}	0.065^{***}	-0.132^{*}	0.003^{***}	-0.028^{***}	−0.008	−0.010	0.003^{+}
Apr.	0.032^{*}	0.102^{***}	0.068^{***}	-0.268^{***}	0.008^{***}	-0.040^{***}	0.004	0.004	0.003
May	0.023^{*}	0.100^{***}	0.055^{***}	-0.114^{*}	0.007^{***}	-0.038^{***}	−0.002	−0.002	−0.004
Jun.	0.033^{***}	0.097^{***}	0.052^{***}	-0.151^{***}	0.010^{***}	-0.025^{***}	−0.004	−0.006	−0.001
Jul.	0.036^{***}	0.076^{***}	0.049^{***}	-0.219^{***}	0.011^{***}	-0.016^{***}	0.002	0.002	0.005
Aug.	0.029^{*}	0.052^{***}	0.038^{***}	-0.239^{***}	0.009^{***}	-0.019^{***}	0.006	0.009	0.004
Sep.	0.020^{*}	0.083^{***}	0.047^{***}	-0.176^{**}	0.006^{***}	-0.017^{***}	−0.014*	-0.017^{*}	−0.001
Oct.	0.025*	0.083^{***}	0.059^{***}	-0.255^{***}	0.005^{***}	-0.021^{***}	−0.004	−0.004	0.002
Nov.	0.031^{*}	0.063^{***}	0.054^{***}	-0.174^{***}	0.002^{***}	-0.034^{***}	−0.004	−0.004	−0.001
Dec.	0.023	0.101^{***}	0.071^{***}	-0.109^{+}	0.001^{***}	-0.029^{***}	-0.018^{**}	-0.013^{**}	−0.001
Crop growing season	0.030^{***}	0.088^{***}	0.054^{***}	-0.195^{***}	0.008^{***}	-0.027^{***}	−0.133	−0.084	0.43
Annual mean or total	0.029^{***}	0.098^{***}	0.066^{***}	-0.132^{***}	0.006^{***}	-0.030^{***}	-2.137^{+}	−1.952	0.41

Note: Symbols represent significance level P according to a Mann-Kendall test: *** means $P \le 0.001$, ** means $P \le 0.01$, * means $P \le 0.05$, and $^{+}$ means $P \le 0.1$. Values without symbols are not significant.

Fig. 1(a) shows that air temperatures, including T_{max}, T_{min}, and T_{ave}, increased from 1954 to 2012. From the 1950s to the 2000s, annual mean T_{max}, T_{min}, and T_{ave} increased by 1.32℃, 4.18℃, and 3.22℃, respectively. The statistical analyses in Table 2 show that the increasing trends in T_{min} and T_{ave} were significant ($P \le 0.001$) for all months and that T_{max} was significant ($P \le 0.05$) for the period from April to December. At the crop growing seasonal and annual time scales, T_{max}, T_{min}, and T_{ave} significantly increased from 1954 to 2012. T_{min} showed the highest rate of increase, ranging from 0.52℃ to 1.27℃ per decade across the twelve months of the year. Increases in T_{min} were 0.88℃ and 0.98℃ per decade for a crop growing season and a year, respectively. Monthly T_{ave} increased at a rate of 0.38℃ to 0.91℃ per decade, and seasonal and annual T_{ave} increased at rates of 0.54℃ and 0.66℃ per decade, respectively. T_{max} had a lower rate of increase than T_{min} or T_{ave}. Similar increasing trends in mean temperature have been reported in southern Spain (rates of 0.16℃ to 0.40℃ per decade) (Espadafor et al. 2011), and rates of 0.2℃ to 0.41℃ per decade have been reported in France (Chaouche et al. 2010). At the global scale, the total temperature increase over the last 100 years from 1906 to 2005 was 0.74℃ (IPCC 2007), with a linear rate of 0.074℃ per decade. This warming climate is likely to lead to increased potential evapotranspiration and increased irrigation needs in regions with low rainfall (Chattopadhyay and Hulme 1997).

Annual mean relative humidity showed a consistent decreasing trend over the past 59 years, as shown in Fig. 1(b). Similarly, in most months (from March to November), monthly mean relative humidity decreased significantly ($P \leq 0.05$) (Table 2). Estimated rates of decrease ranged from 1.09% to 2.68% per decade for monthly mean relative humidity and 1.95% and 1.32% per decade for seasonal and annual relative humidity, respectively. Increasing trends in monthly mean relative humidity were observed for January and February, which offset the decreasing trend during the other months and resulted in a lower rate of decrease for annual mean relative humidity compared with seasonal mean relative humidity. These decreasing trends in relative humidity suggest a shift towards a much drier climate, which may cause a greater atmospheric water demand and hence a larger crop water requirement.

VPD generally increases with increasing temperature and decreasing relative humidity (Allen et al. 1998). Therefore, the observed increasing trend in air temperature (Fig. 1(a)) and decreasing trend in relative humidity (Fig. 1(b)) may result in increased VPD. This inference was confirmed by the increasing VPD trend shown in Fig. 1(c). The statistical analysis in Table 2 shows that a significant increasing trend in VPD was observed in all months, with larger increases (0.08 to 0.11 kPa per decade) from April to August. Rates of increase in seasonal and annual VPD were 0.08 and 0.06 kPa per decade, respectively. The higher rate of increase in seasonal VPD may be due to the high rate of increase during the period from April to August. A higher VPD generally results in a greater evaporation rate. Hence, increased VPD in Hetao will result in an increased rate of crop evapotranspiration.

Wind speed in Hetao decreased gradually from 1954 to 2012 (Fig. 1(d)). The statistical analyses in Table 2 show that significant decreasing trends ($P \leq 0.001$) were found for wind speed for each month, as well as for crop seasonal and annual wind speeds. The rate of decrease for monthly mean wind speed ranged from 0.16 to 0.40 m/s per decade. Higher rates of increase generally occurred from December to May, ranging from 0.28 to 0.40 m/s per decade. In contrast, during the period of most rapid crop development, i.e., between June and August, lower rates of decrease were observed for monthly wind speed of 0.16 to 0.25 m/s per decade, which in turn resulted in a lower rate of decrease (0.27 m/s per decade) at the seasonal time scale compared with the annual time scale (0.30 m/s per decade).

Annual total sunshine hours and solar radiation are illustrated in Fig. 1(e) and 1(f), respectively. Both sunshine hours and solar radiation showed slight decreasing trends. From the 1950s to the 2000s, annual total sunshine hours and radiation decreased by 19 h and 25 MJ/m^2, respectively. Sunshine hours and solar radiation showed decreasing trends during nine out of 12 months of the year (no decreasing trend in April, July, or August) (Table 2). Significant ($P \leq 0.01$) decreasing trends were detected for December through February. During this period, the rates of decrease were the largest of the twelve months, with values of approximately –60 h per decade for sunshine hours and –50 MJ/m^2 per decade for solar radiation. Total sunshine hours decreased at rates of 1.3 and 21 h per decade at the seasonal and annual time scales, respectively. Radiation decreased at rates of 0.8 and 19.5 MJ/m^2 per decade at the seasonal and annual time scales, respectively. The approximately 20-fold increases in the rates of increase of sunshine hours and radiation between the seasonal and annual time scales may be mainly due to the trends for April, July, and August. These increasing trends may have offset the effect of the decreasing trends for May, June, September, and October, resulting in a slight decreasing trend in seasonal sunshine hours and radiation. The rate of decrease of 19.5 MJ/m^2 per decade for annual total radiation, which is equivalent to 0.06 W/m^2 per year, falls into the range of the estimated reduction of 0.51 to 0.05 W/m^2 per year of solar radiation reaching the Earth's surface (Stanhill and Cohen 2001). A reduction in sunshine hours and radiation during the crop growing season could possibly inhibit crop growth and yield because crop biomass linearly increases with the cumulative absorbed photosynthetically active radiation (Daughtry et al. 1992).

Sunshine hours generally depend on cloud cover and the concentration of man-made aerosols and some air pollutants (including SO_2, NO_x, and particulate matter in the atmosphere (Kitsara et al. 2013; Wang et al. 2013). Recent studies have noted that the most probable cause for decreases in sunshine hours or solar radiation is increased concentrations of man-made aerosols and other air pollutants (Stanhill and Cohen 2001; IPCC 2007; Hu and Wang 2008; Liu et al. 2012; Kitsara et al. 2013; Wang et al. 2013).

3.2 Changes in ET_{0R} and ET_{0a}

Fig. 2 shows average annual distributions (1954 to 2012) for daily ET_0, ET_{0R}, and ET_{0a}. Daily ET_0, ET_{0R}, and ET_{0a} showed single-peak annual curves, but the maximum values occurred at different times during the year. Daily ET_0, ET_{0R}, and ET_{0a} increased beginning in January. ET_{0a} was the first to peak, in May, followed by ET_0 in June and ET_{0R} in July. After reaching their respective peak values, all three forms of ET_0 decreased gradually and reached their minimum values in December and January. ET_{0a} was higher than ET_{0R} during the period from January to April, which resulted in a higher contribution rate to ET_0 for ET_{0a} than ET_{0R}.

However, the contribution rate of ET_{0a} decreased from approximately 0.7 in January to 0.5 in May (Fig. 2(b)). During the period from May to October, ET_{0R} was higher than ET_{0a}, and the contribution of ET_{0R} was higher than that of ET_{0a}. The highest contribution rate to ET_0 from ET_{0R} (approximately 0.7) occurred in July. This higher rate may have been due to the higher radiation density, lower wind speed, and higher relative humidity that occurred during this month (Fig. 3). In July, radiation density reached an annual maximum (Fig. 3(a)), indicating that the highest rate of energy-supported evapotranspiration occurred during this month. During the same period, wind speed was at an annual low (Fig. 3(b)), and relative humidity was at an annual high (Fig. 3(c)). These conditions were expected to result in a lower evapotranspiration rate. ET_{0a} appears to make a relatively low contribution to ET_0 in July.

Therefore, during this period, decreasing the radiation load through the use of a shelter or other crop cover would be the most useful method for reducing crop evapotranspiration, but it should be noted that radiation reduction may reduce leaf photosynthesis and lastly affect plant yield.

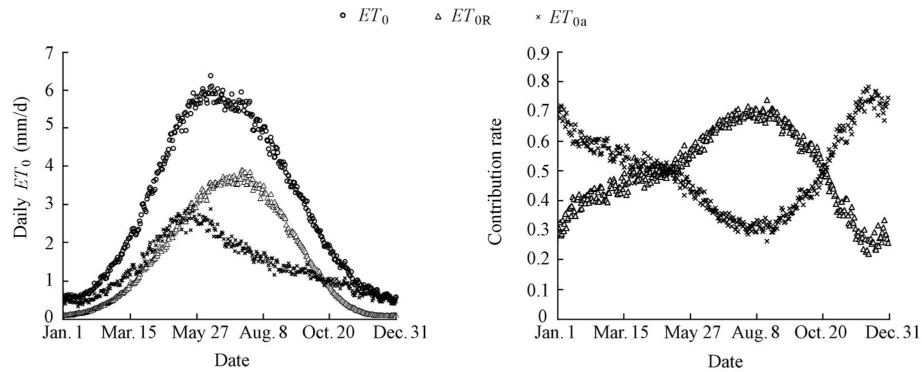

(a) Annual distribution of daily ET_0

(b) Relative contributions of ET_{0R} and ET_{0a}

Fig. 2 Annual distribution of daily ET_0, ET_{0R}, and ET_{0a}

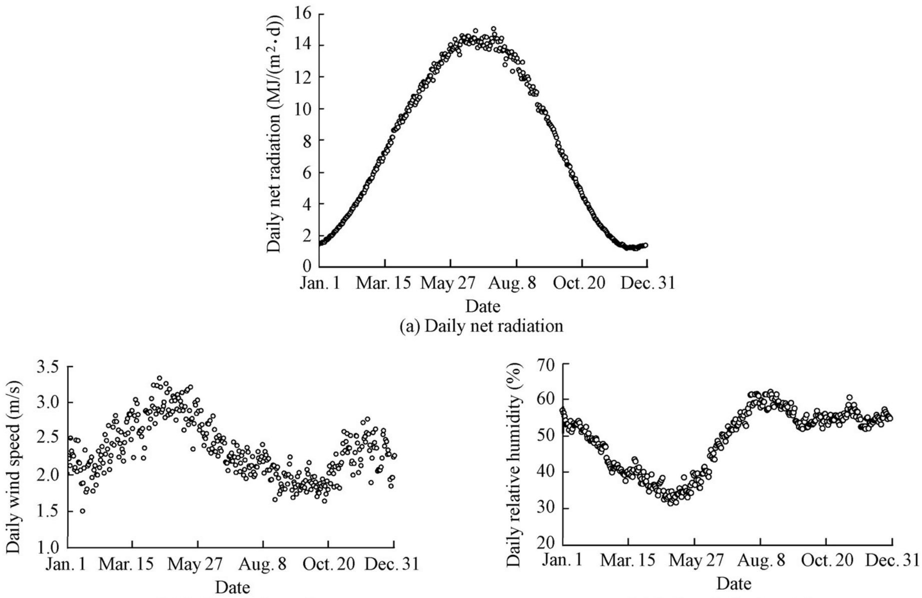

(a) Daily net radiation

(b) Daily wind speed

(c) Daily relative humidity

Fig. 3 Annual distributions of climatic variables

Annual total ET_0 varied from 987 to 1 183 mm, with a mean of 1 095 mm. Seasonal and annual total ET_0 showed a slight increasing trend, with rates of 4.3 and 4.1 mm per decade, respectively (Table 2), but these trends were not significant. For monthly total ET_0, most increasing trends occurred during the crop growing season, and most decreasing trends occurred during the off season. The highest rate of increase was approximately 18 mm per decade, occurring in April. Similar rates of increase in ET_0, ranging from 18 to 35 mm per decade, were reported by Espadafor et al. (2011) for southern Spain. In most regions of China, seasonal and annual ET_0 have shown a tendency to decline over the past 50 years (Gao et al. 2006; Tang et al. 2011; Huo et al. 2013). This variation in ET_0 trends among regions may be due to changes in the dominant climatic factors in each region (Gao et al. 2006; Gong et al. 2006; Huo et al. 2013). Increased ET_0 suggests increased potential for crop evapotranspiration. With low precipitation rates in Hetao, water requirements for irrigation are likely to increase in the future.

While annual ET_0 showed a slight increasing trend (Fig. 4(a)), ET_{0R} and ET_{0a} showed different patterns of change. From 1954 to 2012, annual total ET_{0R} increased significantly ($P \leq 0.001$) at a rate of 15.4 mm per decade. Similarly, the contribution rate of ET_{0R} to total ET_0 also showed a significant ($P \leq 0.001$) increasing trend (Fig. 4(b)). In contrast, annual total ET_{0a} showed a decreasing trend at a rate of –12.5 mm per decade (Fig. 4(a)).

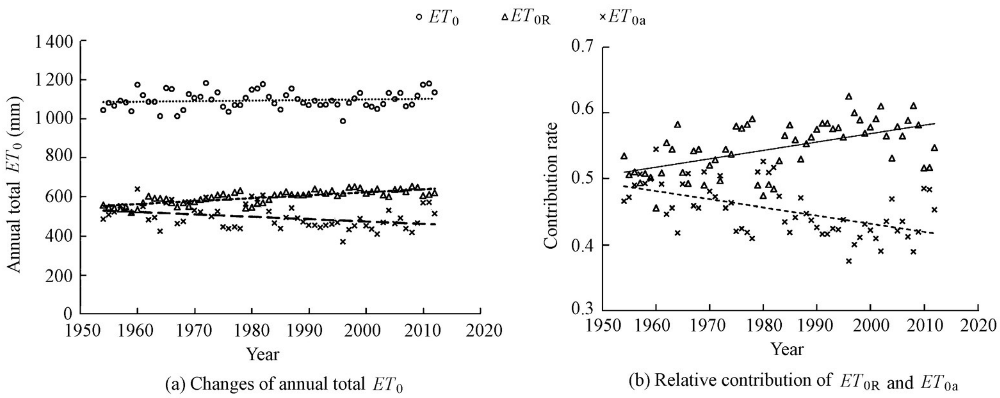

Fig. 4 Multi-year variation of ET_0, ET_{0R}, and ET_{0a} from 1954 to 2012

The mean contribution rate of ET_{0R} to ET_0 averaged 0.55 from 1954 to 2012, indicating a more than 10% contribution as compared to ET_{0a}. In contrast, the annual mean contribution rate of ET_{0R} to ET_0 varied year-to-year (Fig. 4(b)). In the 1950s, the mean contribution rate of ET_{0R} to ET_0 was 0.50, i.e., a 50% contribution to ET_0. After the 1950s, this rate increased linearly, reaching a maximum value of 0.57 in the 2000s (Fig. 4(b)). In contrast, the contribution rate of ET_{0a} to ET_0 decreased from 0.50 in the 1950s to 0.43 in the 2000s. The observed variation in the contributions of ET_{0R} and ET_{0a} to ET_0 may have been mainly due to changes in climatic variables over the past 59 years from 1954 to 2012. Solar radiation showed a slight decrease (rate of 25.4 MJ/m^2 per year) over this period, amounting to a 0.4% decrease from the 1950s to the 2000s). This may have had a minor effect on ET_{0R}. During the same period, wind speed decreased by 40%, mean air temperature increased from 5.73℃ to 8.95℃, and the VPD increased by 30%. Eq. (3) shows a negative relationship between ET_{0R} and wind speed. Therefore, the reduction in wind speed clearly may cause an increase in ET_{0R}. Eq. (4) shows that both the wind speed and VPD are positively linearly related to ET_{0a}. Therefore, a 40% decrease in wind speed (Fig. 1(d)) partly makes up the 30% increases in VPD (Fig. 1(c)) and lastly results in a decrease in ET_{0a}.

3.3 Sensitivity of ET_0 to changes in climatic variables

The climatic variables included in this study showed either increasing or decreasing trends over the past 59 years. The influence of each variable on ET_0 was estimated using the sensitivity analysis method described in section 2.2.2. The sensitivity analysis was performed at the monthly, crop growing seasonal (from April to October), and annual scales. Daily mean data for each month were averaged over the 1950s and the 2000s for each climatic variable. The results of the sensitivity analysis are shown in Table 3.

Table 3 Daily ET_0 variation at monthly, seasonal, and annual time scales and associated changes in climatic variables from 1950s to 2000s

Time period	Changes in ET_0 in 2000s		Changes in ET_0 corresponding to changes of different variables							
			T_{ave}		Relative humidity		Wind speed		Sunshine hours	
	Rate of change* (mm/d)	Percent change** (%)	Rate of change*** (mm/d)	Percent change** (%)	Rate of change*** (mm/d)	Percent change** (%)	Rate of change*** (mm/d)	Percent change** (%)	Rate of change*** (mm/d)	Percent change** (%)
Jan.	−0.123	−19.1	0.073	11.3	−0.055	−8.5	−0.133	−20.6	0.000	0.0
Feb.	0.003	0.2	0.228	21.4	−0.024	−2.3	−0.148	−13.9	0.002	0.1
Mar.	0.279	14.1	0.323	16.2	0.108	5.4	−0.115	−5.8	0.016	0.8
Apr.	0.563	15.6	0.627	17.4	0.126	3.5	−0.233	−6.5	0.154	4.3
May	0.208	3.9	0.651	12.2	0.201	3.8	−0.497	−9.3	0.056	1.0
Jun.	0.384	6.7	0.480	8.4	0.346	6.1	−0.384	−6.7	0.138	2.4
Jul.	0.403	7.6	0.375	7.1	0.328	6.2	−0.238	−4.5	0.089	1.7
Aug.	0.703	17.2	0.373	9.1	0.456	11.1	−0.161	−3.9	0.219	5.4
Sep.	−0.053	−1.6	0.236	7.0	0.095	2.8	−0.224	−6.6	−0.071	−2.1
Oct.	0.099	4.8	0.396	19.1	−0.036	−1.8	−0.211	−10.2	0.048	2.3
Nov.	0.111	11.1	0.220	22.1	0.078	7.8	−0.121	−12.1	0.000	0.0
Dec.	0.083	15.0	0.122	22.1	0.053	9.7	−0.062	−11.3	0.000	0.0
Crop growing season	0.330	7.8	0.448	10.6	0.216	5.1	−0.278	−6.6	0.090	2.1
Non-growing season	0.071	6.7	0.193	18.4	0.032	3.0	−0.116	−11.0	0.004	0.4
Annual	0.222	7.7	0.342	11.8	0.140	4.8	−0.211	−7.3	0.054	1.9

Note: * Values in this column represent absolute changes in ET_0 caused by climate change. ** Values in this column represent change percent of ET_0 caused by changes in the corresponding climatic variable. *** Values in this column represent relative changes in ET_0 caused by changes in the corresponding climatic variable.

Increased mean air temperature resulted in a great increase in ET_0, as shown in Table 3. Compared with mean daily ET_0 for each month for the 1950s, the change in ET_0 due to changes in air temperature in the 2000s ranged from 0.07 to 0.65 mm/d. The largest changes occurred in April and May, with increments of change higher than 0.60 mm/d, followed by June, October, and July, with changes above 0.37 mm/d. The lowest increments of change were found for December and January, with values of less than 0.15 mm/d. Mean increments of change in daily ET_0 caused by increases in temperature were 0.45 and 0.34 mm/d at the seasonal and annual time scale, respectively, for a percent change of 10.6% and 11.8%. The higher increases during the crop growing season were mainly due to the greater increases in air temperature that occurred from April to October.

The decrease in relative humidity during most months over the past 59 years resulted in increases in ET_0 during the corresponding months. The largest increase in daily ET_0 caused by decreased relative humidity was 0.46 mm/d in August, followed by increases in June of 0.35 mm/d. Seasonal and annual increases in ET_0 caused by decreases in relative humidity were 0.22 and 0.14 mm/d, respectively.

Over the past 59 years, decreasing wind speed has caused decreases in daily ET_0 at the monthly, seasonal, and annual time scales. The highest rate of decrease in ET_0 as a result of a decrease in wind speed was 0.50 mm/d in May, followed by 0.38 mm/d in June. Decreases in ET_0 at rates between 0.2 and 0.3 mm/d occurred in April, July, September, and October. At the seasonal and annual time scales, ET_0 decreased at a rate of 0.28 and 0.21 mm/d, respectively.

Table 3 shows that only small rates of change (0.09 and 0.05 mm/d) were observed in seasonal and annual ET_0 caused by increases in sunshine hours. These results suggest that ET_0 in Hetao is not sensitive to changes in sunshine hours.

Mean daily ET_0 resulting from changes in climatic variables increased in most months. The largest increase in daily ET_0 was 0.70 mm/d in August, followed by April, July, June, and March, with increases of 0.56, 0.40, 0.38, and 0.28 mm/d, respectively. A decreasing trend in ET_0 was observed in January (–0.12 mm/d). This may have been mainly due to the wind speed (–0.13 mm/d) and relative humidity (–0.06 mm/d). Over the past 59 years, mean daily ET_0 increased by 0.33 and 0.22 mm/d (total increases of 7.8% and 7.7%) at seasonal and annual time scales, respectively.

Of the four climatic variables evaluated in this study, mean temperature was the primary factor driving changes in ET_0 over the past 59 years. On an annual basis, changes in mean temperature resulted in an increase in daily ET_0 of 0.34 mm/d (a total increase of 11.8%). The next two most important factors were wind speed (–0.21 mm/d; –7.3%) and relative humidity (0.14 mm/d; 4.8%). Sunshine hours had minor effects on ET_0 over the past 59 years.

Generally, the sensitivity of ET_0 to climatic variables varies among regions due to their different climatic characteristics. In the arid region of Northwest China, Huo et al. (2013) found that ET_0 was most sensitive to wind speed, followed by relative humidity, temperature, and radiation. This finding is similar to the results presented in this study. Huo et al. (2013) suggested that the relatively large effect of wind speed on ET_0 in this arid region could be explained by the lower amount of water vapor carried by the wind in drier climates compared with more humid climates. In contrast, in the relatively humid region of the Haihe River Basin in northern China, Tang et al. (2011) found that ET_0 was most sensitive to temperature and radiation, which caused changes in ET_0 of 2.5 and –1.2 mm/year, respectively. In most cases, temperature, wind speed, and sunshine hours were the key factors in ET_0 change (Espadafor et al. 2011; Goyal 2004; Liang et al. 2010; Tabari et al. 2011; Tanaka et al. 2008; Tang et al. 2011). The reason for this may be due to the fact that these climatic variables have changed greatly in the past few centuries. For example, global air temperatures from 1906 to 2005 increased by 0.74℃, based on observational data (IPCC 2007), and the continued greenhouse gas emissions at or above current rates are expected to cause further warming during the 21st century (IPCC 2007). McVicar et al. (2012) analyzed 148 studies that reported trends in terrestrial winds from across the globe (with uneven and incomplete spatial distribution and different periods of measurement) and found that the average trend of wind speed was –0.014 m/s per year for studies with more than 30 sites and observational data for a period of more than 30 years. They also found that this decreasing trend in wind speed was the main contributor to declining evaporation rates. In most parts of China, clear decreasing trends in solar radiation have been observed (Tang et al. 2011; Zhang et al. 2011b; Wang et al. 2013). Increased air pollution and aerosols in highly urbanized regions, in addition to global climate change, are the main driving factors causing decreases in net radiation (Stanhill and Cohen 2001; Yang et al. 2009; Zhang et al. 2011; Wild 2009, 2012).

4 Conclusions

(1) The following trends were observed in climatic variables at the Linhe Station of Hetao from 1954 to 2012: maximum, minimum, and mean daily air temperatures increased significantly, relative humidity and wind speed decreased dramatically, and sunshine hours and solar radiation decreased slightly. The vapor pressure deficit has increased over the past 59 years, mainly due to increases in temperature and decreases in relative humidity.

(2) The contribution of radiative evapotranspiration to daily total ET_0 increased from 0.50 in the 1950s to 0.57 in the 2000s. The contribution of aerodynamic evaporation decreased from 0.50 to 0.43. At an annual scale, the higher ET_0 rate during the crop growing season was mainly due to the increased radiative component of ET_0.

(3) The sensitivity analysis showed that ET_0 at the Linhe Station of Hetao is primarily sensitive to mean daily air temperature (11.8%), followed by wind speed (−7.3%), and relative humidity (4.8%). Changes in sunshine hours have had a minor effect on ET_0 over the past 59 years.

References

Allen, R. G., Pereira, L. S., Raes, D., and Smith, M. 1998. *Crop Evapotranspiration-Guidelines for Computing Crop Water Requirements-FAO Irrigation and Drainage Paper 56*. Rome: Food and Agriculture Organization of the United Nations (FAO).

Bates, B. C., Kundzewicz, Z. W., Wu, S., and Palutikof, J. 2008. *Climate Change and Water*. Geneva: Intergovernmental Panel on Climate Change (IPCC) Secretariat.

Chaouche, K., Neppel, L., Dieulin, C., Pujol, N., Ladouche, B., Martin, E., Salas, D., and Caballero, Y. 2010. Analyses of precipitation, temperature and evapotranspiration in a French Mediterranean region in the context of climate change. *Comptes Rendus Geoscience*, 342(3), 234-243. [doi:10.1016/j.crte.2010.02.001]

Chattopadhyay, N., and Hulme, M. 1997. Evaporation and potential evapotranspiration in India under conditions of recent and future climate change. *Agricultural and Forest Meteorology*, 87(1), 55-73. [doi:10.1016/S0168-1923(97)00006-3]

Darshana, P. A., and Pandey, R. P. 2013. Analysing trends in reference evapotranspiration and weather variables in the Tons River Basin in Central India. *Stochastic Environmental Research and Risk Assessment*, 27(6), 1407-1421. [doi:10.1007/s00477-012-0677-7]

Daughtry, C. S. T., Gallo, K. P., Goward, S. N., Prince, S. D., and Kustas, W. P. 1992. Spectral estimates of absorbed radiation and phytomass production in corn and soybean canopies. *Remote Sensing of Environment*, 39(2), 141-152. [doi:10.1016/0034-4257(92)90132-4]

Espadafor, M., Lorite, I. J., Gavilán, P., and Berengena, J. 2011. An analysis of the tendency of reference evapotranspiration estimates and other climate variables during the last 45 years in Southern Spain. *Agricultural Water Management*, 98(6), 1045-1061. [doi:10.1016/j.agwat.2011.01.015]

Fan, Z. X., and Thomas, A. 2013. Spatiotemporal variability of reference evapotranspiration and its contributing climatic factors in Yunnan Province, SW China, 1961-2004. *Climatic Change*, 116(2), 309-325. [doi:10.1007/s10584-012-0479-4]

Gao, G., Chen, D., Ren, G., Chen, Y., and Liao, Y. 2006. Spatial and temporal variations and controlling factors of potential evapotranspiration in China: 1956-2000. *Journal of Geographical Sciences*, 16(1), 3-12. [doi:10.1007/s11442-006-0101-7]

Gong, L. B., Xu, C. Y., Chen, D. L., Halldin, S., and Chen, Y. D. 2006. Sensitivity of the Penman-Monteith reference evapotranspiration to key climatic variables in the Changjiang (Yangtze River) basin. *Journal of Hydrology*, 329(3-4), 620-629. [doi:10.1016/j.jhydrol.2006.03.027]

Goyal, R. K. 2004. Sensitivity of evapotranspiration to global warming: A case study of arid zone of Rajasthan (India). *Agricultural Water Management*, 69(1), 1-11. [doi:10.1016/j.agwat.2004.03.014]

Hamed, K. H. 2008. Trend detection in hydrologic data: The Mann-Kendall trend test under the scaling hypothesis. *Journal of Hydrology*, 349(3-4), 350-363. [doi:10.1016/j.jhydrol.2007.11.009]

Haskett, J. D., Pachepsky, Y. A., and Acock, B. 2000. Effect of climate and atmospheric change on soybean water stress: A study of Iowa. *Ecological Modeling*, 135(2-3), 265-277. [doi:10.1016/S0304-3800(00)00369-0]

Hu, Q. F., and Wang, Y. 2009. Impact assessment of climate change and human activities on annual highest water level of Taihu Lake. *Water Science and Engineering*, 2(1), 1-15. [doi:10.3882/j.issn.1674-2370.2009.01.001]

Huntington, T. G. 2006. Evidence for intensification of the global water cycle: Review and synthesis. *Journal of Hydrology*, 319(1-4), 83-95. [doi:10.1016/j.jhydrol.2005.07.003]

Huo, Z. L., Dai, X. Q., Feng, S. Y., Kang, S. Z., and Huang, G. H. 2013. Effect of climate change on reference evapotranspiration and aridity index in arid region of China. *Journal of Hydrology*, 492(7), 24-34. [doi:10.1016/j.jhydrol.2013.04.011]

Intergovernmental Panel on Climate Change (IPCC). 2007. *Climate Change 2007: Synthesis Report*. Geneva: IPCC.

Irmak, S., Kabenge, I., Skaggs, K. E., and Mutiibwa, D. 2012. Trend and magnitude of changes in climate variables and reference evapotranspiration over 116-yr period in the Platte River Basin, central Nebraska-USA. *Journal of Hydrology*, 420-421, 228-244. [doi:10.1016/j.jhydrol.2011.12.006]

Kitsara, G., Papaioannou, G., Papathanasiou, A., and Retalis, A. 2013. Dimming/brightening in Athens: Trends in sunshine duration, cloud cover and reference evapotranspiration. *Water Resources Management*, 27(6), 1623-1633. [doi:10.1007/s11269-012-0229-4]

Kousari, M. R., Zarch, M. A. A., Ahani, H., and Hakimelahi, H. 2013. A survey of temporal and spatial reference crop evapotranspiration trends in Iran from 1960 to 2005. *Climatic Change*, 120(1-2), 277-298.

[doi:10.1007/s10584-013-0821-5]

Liang, L. Q., Yan, M. H., Deng, W., and Li, L. J. 2006. Change of reference crop evapotranspiration from West Songnen Plain. *Progress in Geography*, 25(3), 22-31. (in Chinese)

Liang, L. Q., Li, L. J., Zhang, L., Li, J. Y., Jiang, D. J., Xu, M. X., and Song, W. X. 2008. Sensitivity of the reference crop evapotranspiration in growing season in the West Songnen Plain. *Transaction of Chinese Society of Agricultural Engineering*, 24(5), 1-5. (in Chinese)

Liang, L. Q., Li, L. J., and Liu, Q. 2010. Temporal variation of reference evapotranspiration during 1961-2005 in the Taoer River basin of Northeast China. *Agricultural and Forest Meteorology*, 150(2), 298-306. [doi:10.1016/j.agrformet.2009.11.014]

Liu, C. M., Zhang, D., Liu, X. M., and Zhao, C. S. 2012. Spatial and temporal change in the potential evapotranspiration sensitivity to meteorological factors in China (1960-2007). *Journal of Geographical Sciences*, 22(1), 3-14. [doi:10.1007/s11442-012-0907-4]

Liu, H. J., Li, Y., Tanny, J., Zhang, R. H., and Huang, G. H. 2014. Quantitative estimation of climate change effects on potential evapotranspiration in Beijing during 1951-2010. *Journal of Geographical Sciences*, 24(1), 93-112. [doi:10.1007/s11442-014-1075-5]

McVicar, T. R., Roderick, M. L., Donohue, R. J., Li, L. T., Van Niel, T. G., Thomas, A., Grieser, J., Jhajharia, D., Himri, Y., Mahowald, N. M., et al. 2012. Global review and synthesis of trends in observed terrestrial near-surface wind speeds: Implications for evaporation. *Journal of Hydrology*, 416-417, 182-205. [doi:10.1016/j.jhydrol.2011.10.024]

Möller, M., Tanny, J., Li, Y., and Cohen, S. T. 2004. Measuring and predicting evapotranspiration in an insect-proof screenhouse. *Agricultural and Forest Meteorology*, 127(1-2), 35-51. [doi:10.1016/j.agrformet.2004.08.002]

Ren, J. L., Li, Q. F., Yu, M. X., and Li, H. Y. 2012. Variation trends of meteorological variables and their impacts on potential evaporation in Hailar region. *Water Science and Engineering*, 5(2), 137-144. [doi:10.3882/j.issn.1674-2370.2012.02.002]

Rim, C. 2009. The effects of urbanization, geographical and topographical conditions on reference evapotranspiration. *Climatic Change*, 97(3-4), 483-514. [doi:10.1007/s10584-009-9618-y]

Sen, P. K. 1968. Estimates of the regression coefficient based on Kendall's Tau. *Journal of the American Statistical Association*, 63(324), 1379-1389. [doi:10.1080/01621459.1968.10480934]

Stanhill, G., and Cohen, S. 2001. Global dimming: A review of the evidence for a widespread and significant reduction in global radiation with discussion of its probable causes and possible agricultural consequences. *Agricultural and Forest Meteorology*, 107(4), 255-278. [doi:10.1016/S0168-1923(00)00241-0]

Tabari, H., Marofi, S., Aeini, A., Talaee, P. H., and Mohammadi, K. 2011. Trend analysis of reference evapotranspiration in the western half of Iran. *Agricultural and Forest Meteorology*, 151(2), 128-136. [doi:10.1016/j.agrformet.2010.09.009]

Tabari, H., Nikbakht, J., and Talaee, P. H. 2012. Identification of trend in reference evapotranspiration series with serial dependence in Iran. *Water Resources Management*, 26(8), 2219-2232. [doi:10.1007/s11269-012- 0011-7]

Talaee, P. H., Some, B. S., and Ardakani, S. S. 2014. Time trend and change point of reference evapotranspiration over Iran. *Theoretical and Applied Climatology*, 116(3-4), 639-647. [doi:10.1007/s00704-013-0978-x]

Tanaka, N., Kume, T., Yoshifuji, N., Tanaka, K., Takizawa, H., Shiraki, K., Tantasirin, C., Tangtham, N., and Suzuki, M. 2008. A review of evapotranspiration estimates from tropical forests in Thailand and adjacent regions. *Agricultural and Forest Meteorology*, 148(5), 807-819. [doi:10.1016/j.agrformet.2008.01.011]

Tang, B., Tong, L., Kang, S. Z., and Zhang, L. 2011. Impacts of climate variability on reference evapotranspiration over 58 years in the Haihe river basin of north China. *Agricultural Water Management*, 98(10), 1660-1670. [doi:10.1016/j.agwat.2011.06.006]

Wang, Y. W., Yang, Y. H., Han, S. M., Wang, Q. X., and Zhang, J. H. 2013. Sunshine dimming and brightening in Chinese cities (1955-2011) was driven by air pollution rather than clouds. *Climate*

Research, 56(1), 11-20. [doi:10.3354/cr01139]

Wild, M. 2009. Global dimming and brightening: A review. *Journal of Geophysical Research: Atmospheres* (1984-2012), 114(D10). [doi:10.1029/2008JD011470]

Wild, M. 2012. Enlightening global dimming and brightening. *Bulletin of the American Meteorological Society*, 93(1), 27-37. [doi:10.1175/BAMS-D-11-00074.1]

Xu, C. Y., Gong, L. B., Jiang, T., Chen, D. L., and Singh, V. P. 2006. Analysis of spatial distribution and temporal trend of reference evapotranspiration and pan evaporation in Changjiang (Yangtze River) catchment. *Journal of Hydrology*, 327(1-2), 81-93. [doi:10.1016/j.jhydrol.2005.11.029]

Xu, X., Huang, G. H., Qu, Z. Y., and Pereira, L. S. 2010. Assessing the groundwater dynamics and impacts of water saving in the Hetao Irrigation District, Yellow River basin. *Agricultural Water Management*, 98(2), 301-313. [doi:10.1016/j.agwat.2010.08.025]

Yang, Y. H., Zhang, Z. Y., and Xiang, X. Y. 2009. Spatial variation of reference crop evapotranspiration on Tibetan Plateau. *Water Science and Engineering*, 2(1), 112-120. [doi:10.3882/j.issn.1674-2370.2009.01.011]

Yu, L. L., Xia, Z. Q., Li, J. K., and Cai, T. 2013. Climate change characteristics of Amur River. *Water Science and Engineering*, 6(2), 131-144. [doi:10.3882/j.issn.1674-2370.2013.02.002]

Zhang, D., Liu, X. M., and Hong, H. Y. 2013. Assessing the effect of climate change on reference evapotranspiration in China. *Stochastic Environmental Research and Risk Assessment*, 27(8), 1871-1881. [doi:10.1007/s00477-013-0723-0]

Zhang, Q., Xu, C. Y., Chen, Y. D., and Ren, L. L. 2011a. Comparison of evapotranspiration variations between the Yellow River and Pearl River basin, China. *Stochastic Environmental Research and Risk Assessment*, 25(2), 139-150. [doi:10.1007/s00477-010-0428-6]

Zhang, X. Y., Chen, S. Y., Sun, H. Y., Shao, L. W., and Wang, Y. Z. 2011b. Changes in evapotranspiration over irrigated winter wheat and maize in North China Plain over three decades. *Agricultural Water Management*, 98(6), 1097-1104. [doi:10.1016/j.agwat.2011.02.003]

(Edited by Yun-li YU)